Tellus B (1998), 50, 205–223
Printed in UK–all rights reserved

TELLUS
ISSN 0280–6495

A regional scale multi-layer model for the calculation of long-term transport and deposition of air pollution in Europe

By ERIK BERGE[1] and HUGO A. JAKOBSEN[2], [1]*EMEP MSC-W, The Norwegian Meteorological Institute, P.O. Box 43, Blindern, N-0313 Oslo, Norway*

(Manuscript received 19 June 1997; in final form 22 January 1998)

ABSTRACT

In this paper, we present a multi-layer Eulerian model aiming at calculating the long-term source-receptor relationships of air pollutants at the European regional scale. As a first approach, results from annual transport and deposition of sulphur dioxide and sulphate is given in this study. The model is however formulated in order to facilitate further studies of other air pollutants in the future. The model takes advantage of new detailed information on meteorology and emissions to the air in a 50 km × 50 km resolution. The model is formulated in a terrain following coordinate system, and a higher order numerical advection scheme is employed in order to reduce numerical diffusion. A simple linear parameterization scheme for sulphur dispersion and deposition is implemented. The wet scavenging is directly coupled to the release of precipitation in each model layer. The model has been employed for a full year simulations for sulphur transport and deposition in Europe. Model comparison with 60–70 measuring stations in Europe show realistic values for SO_2 and sulphate in air and wet deposition of sulphate. Averaged of all stations the model deviates by only a few percent from the measured average. However, at individual stations the differences between the model and the measurements are sometimes larger, but seldom more than a factor of two difference is encountered. Further, comparison with a two-dimensional Lagrangian single layer model shows qualitatively good agreements. The most pronounced improvement encountered by use of the multi-level model are the increased wet deposition rates in remote areas, well in accordance with the measurements. This is ascribed to the improved description of the transport and wet scavenging processes by using a multi-layer rather than a single layer approach.

1. Introduction

During the last 20 years, several models have been developed with the purpose of analyzing long term regional scale transport and deposition of air pollutants in Europe. Two-dimensional receptor oriented Lagrangian models were first used under the OECD-project (Eliassen, 1978) and later in the EMEP* program (Eliassen and Saltbones, 1983). This model type has quite successfully been used to estimate annual concentrations and depositions of acidifying sulphur and nitrogen compounds (Hov et al., 1988; Iversen, 1993; Barrett et al., 1995), as well as long-term concentrations of boundary layer ozone (Simpson, 1993, 1996). They are designed to simulate pro-

[1] Corresponding author.
E-mail: erik.berge@dnmi.no
[2] Present affiliation: Department of Chemical Engineering, Norwegian University of Science and Technology, N-7034 Trondheim, Norway.
E-mail: jakobsen@chembio.ntnu.no

* EMEP = European Monitoring and Evaluation Program.

cesses inside the atmospheric boundary layer (ABL) with 150 km × 150 km horizontal resolution. An important assumption in these models is that the emitted air pollutants are well mixed up to the top of the boundary layer. This assumption has been justified by the coarse horizontal resolution employed, since well mixed conditions are generally fulfilled before horizontal transport longer than 150 km has taken place. Models with finer horizontal resolution with several layers inside the ABL in order to describe the initial dispersion of air pollutants, do not have to presume such well mixed conditions. A multi-layer approach is also needed in order to describe the effects of windshear, vertical exchange between the ABL and the free troposphere, and free tropospheric cloud chemistry.

Several regional scale multi-layer Eulerian models have been developed with the purpose of analyzing regional scale transport and deposition of air pollutants. The most well-known North American models are the RADM (Chang et al., 1987; McHenry and Dennis, 1994), the ADOM (Venkatram et al., 1992) and the STEM-II model (Carmichael et al., 1986, 1991). In Europe, the EURAD model which is based on the RADM model has been described and evaluated by Hass et al. (1993). The above-mentioned multi-level models are developed with a large degree of complexity in both the gas and liquid phase chemistry, and they have so far been employed only in short term studies (days up to weeks) since their complexity has prohibited applications to longer term simulations.

There are however clear needs for more detailed long term information on the horizontal and vertical distribution of the air pollution. This will aim at a better understanding of regional scale air pollution problems, and an improvement of the quantification of the transboundary air pollution fluxes between different countries and regions. Such data is of large importance for Integrated Assessment Modeling and the negotiations on emission reduction protocols (Amann and Klaasen, 1995). In response to these requirements a development of a regional scale (50 km × 50 km horizontal resolution) multi-layer model has been initiated under the EMEP program. The aim of this paper is to present a description and analyze results of this new model.

As a part of this development a high quality meteorological data base has been established. A dedicated version of the Numerical Weather Prediction Model at the Norwegian Weather Service has been set up to provide complete meteorological data of 50 km horizontal resolution and for a large number of layers in the vertical direction. Furthermore, the development is up to now concentrated on simple chemical schemes including only sulphur dioxide and sulphate, while more elaborated transport formulations are employed. The model is formulated in order to facilitate the future inclusion of other chemical species. Annual model calculations for sulphur compounds are presented for a full year in Europe in this paper. The model results are evaluated by use of measurements and a comparison with a simpler two-dimensional Lagrangian model, and finally the sulphur budgets are integrated over the entire model domain.

2. Model description

2.1. The model equations

The equations are formulated in the same horizontal and vertical grid as the meteorological data (Section 3). Hence, a normalized vertical pressure coordinate (the sigma coordinate) together with a polar stereographic projection true at 60°N are employed. If we let ψ denote the mixing ratio (kg/kg-air) of any pollutant, the continuity equation may be written

$$\frac{\partial}{\partial t}(\psi p^*) = -m^2 \nabla_H \cdot \left(\frac{\boldsymbol{V}_H}{m} (\psi p^*) \right) - \frac{\partial}{\partial \sigma} (\dot{\sigma} \psi p^*) + \left[\frac{g}{p^*} \right]^2 \frac{\partial}{\partial \sigma} \left[\rho^2 K_z \frac{\partial}{\partial \sigma} (\psi p^*) \right] + \frac{p^*}{\rho} S . \quad (1)$$

The first two terms on the right hand side represent a flux divergence formulation of the advective transport. $\boldsymbol{V}_H$ and ∇_H are the horizontal wind vector and del operator respectively, and m is the map factor on a polar stereographic map projection. The vertical coordinate, σ, is defined as

$$\sigma = \frac{p - p_T}{p^*}, \quad (2)$$

where $p^* = p_S - p_T$ and p, p_S and p_T are the pressure at level σ, the surface pressure and the pressure at

the top of the model atmosphere respectively. p_T equals 100 hPa in the model. The vertical velocity, $\dot{\sigma}$, equals $d\sigma/dt$. The 3rd term on the right-hand side of eq. (1) represents the vertical eddy diffusion where g, ρ and K_z are the gravitational acceleration, air density and vertical eddy diffusion coefficient respectively. Horizontal eddy diffusion is not included in the model. S describes the other chemical and/or physical source or sink terms. The present model version employs 20 layers in the vertical (see Subsection 3.1 for further details).

2.2. *Advection*

An important aspect of Eulerian models is the numerical solution of the advective part of eq. (1). Since the advection for components with a lifetime of one to several days often is the largest term in eq. (1), the related errors must be considered carefully (see for example Rood, 1987; Dabdub and Seinfeld, 1994). Inevitably, some numerical diffusion or dispersion are associated with the numerical solution of the advection equation. In the present model we have chosen to use the so-called Bott-scheme (Bott, 1989a, b). The scheme is mass conserving and positive definite which are important features for long-term regional scale modeling. The scheme has been extensively tested and evaluated and the conclusion is that it represents a good compromise between accuracy and computational cost for a three-dimensional model (Berge and Kristjansson, 1992; Dabdub and Seinfeld, 1994). In the present model, we utilize a fourth order version of the Bott-scheme in the horizontal direction. In the vertical direction a 2nd order version applicable to variable grid distances is employed.

2.3. *Vertical diffusion*

The formulation of the surface fluxes is based on the Monin–Obukhov similarity theory. The vertical exchange coefficient, K_z, is derived from the surface drag coefficient as described in Louis (1979). Above the surface layer, in the atmospheric boundary layer (ABL) and in the free troposphere, the vertical diffusivities are derived from the empirical formulas of Blackadar (1979) where the mixing length and the local bulk Richardson number are the most important parameters. The turbulent mixing length, l, is essentially the original given by Prandtl (1942) with some minor parameter modifications (Iversen and Nordeng, 1987). It equals $k \cdot z$ for $z < z_m$ and k/z_m for $z > z_m$ where $k = 0.35$ (Von Karman's constant), z is the height above the ground and $z_m = 200$ m. Since the numerical advection scheme is somewhat diffusive the horizontal diffusion has not been included. However, in the vertical, the relative importance of the numerical diffusion is smaller in particular close to the surface where the vertical velocities are small.

2.4. *Sulphur chemistry*

The first model evaluation is carried out with sulphur components for the following reasons. The sulphur chemistry can be parameterized in a simple way and it is well documented in literature, it requires relatively small computer resources compared with the inclusion of any more detailed atmospheric chemistry, a substantial amount of sulphur measurements are available and the emissions have up to now been among the best documented.

The parameterization of the sulphur chemistry follows Eliassen and Saltbones (1983), and it describes the oxidation from SO_2 to particulate sulphate in air. The oxidation rate, k_t (s^{-1}), is given by

$$k_t = 3 \cdot 10^{-6} + 2 \cdot 10^{-6} \sin\left[2\pi\left(\frac{\tau - \tau_0}{\tau_a}\right)\right], \qquad (3)$$

where τ is the time of the year, τ_0 is 80 days and τ_a is one year.

This model reaction parameterizes all possible oxidation pathways of SO_2 including gas phase reactions with OH and liquid phase reactions with H_2O_2. In addition, it is assumed that 5% of the sulphur emissions are in the form of particulate sulphate. The loss of mass of SO_2 due to chemical transformation is calculated including the following sink term in the component continuity equation

$$S_{SO_2,\,chem} = -C_{SO_2} \cdot k_t \qquad (4)$$

where C_{SO_2} is the concentration of SO_2 (kg m^{-3}).

In the component continuity equation for sulphate (SO_4^{2-}) the same reaction term is used as a source term (i.e. with opposite sign).

2.5. Dry deposition

The dry deposition velocities for the sulphur compounds can be determined experimentally at a height of about 1 m above the surface. The effective dry deposition velocity, v_h, applicable to the concentrations at the lowest model level at approximately 45 m (assumed to be the top of the surface layer) is then estimated based on the following assumptions. In the constant flux layer the turbulent flux densities are constant, and as indicated in Fig. 1 we have the following relations:

$$v_S \cdot C_{AS} = v_h \cdot C_{Ah} = C_H |\boldsymbol{v}_H| (C_{Ah} - C_{AS}), \quad (5)$$

where v_s is the dry deposition velocity at 1 m, C_{AS} is the concentration of constituent A at 1 m C_{Ah} is the concentration of A at the top of the SBL (i.e., at the lowest model level, $z = h_s$), C_H is the drag coefficient (described later), and $\boldsymbol{v}_H$ is the horizontal wind speed at the lowest model level.

Substituting the unknown C_{AS} concentration, we obtain an expression for the unknown dry deposition velocity at the top of the SBL ($z = h_S$):

$$v_h = \frac{v_S}{\left[1 + \dfrac{v_S}{C_H |\boldsymbol{v}_H|}\right]}. \quad (6)$$

The application and evaluation of this formulation of v_h is encountered in for example Berge (1990) and Tarrason and Iversen (1992). The drag coefficient in the surface layer is calculated from Monin–Obukhov similarity theory by using the Louis (1979) type of functions to include the effect of stability as given by:

$$C_H |\boldsymbol{v}_H| = \begin{cases} u_*^2/(0.74 \cdot |\boldsymbol{v}_H|) \\ \qquad \text{for } |H_D| \leqslant 0.1 \qquad \text{W m}^{-2} \\ 1 \Big/ \left(p_S \left| \dfrac{\theta_{k=20}/\theta_S - 1}{(R/C_P) H_D} \right| \right) \\ \qquad \text{for } |H_D| > 0.1 \qquad \text{W m}^{-2} \end{cases} \quad (7)$$

where u_* is the friction velocity, $\theta_{k=20}$ is the potential temperature at the lowest model level ($k = 20$), θ_S is the potential temperature at the ground level (i.e., $z = 2$ m) and H_D is the turbulent heat flux density in the SBL.

The loss of mass of component A due to dry deposition is calculated including the following sink term in the component continuity equation

$$S_{A,\ \text{dry dep}} = -C_A \cdot \frac{v_h}{\Delta z}, \quad (8)$$

where Δz is the thickness of the lowest model layer.

The dry deposition velocity for SO_2 at 1 m, v_S, is set equal to 0.8 cm s^{-1} over sea and it is somewhat lower over land depending on the latitude and the time of the year (see Barrett et al. (1995) for further details). For particulate sulphate, SO_4^{2-}, the deposition velocity at 1 m is set equal to 0.1 cm s^{-1} everywhere.

The exchange of the pollutant between the atmosphere and soil, vegetation or water is governed both by transfer in the gas-phase and by sorption at the surface, which is assumed to be

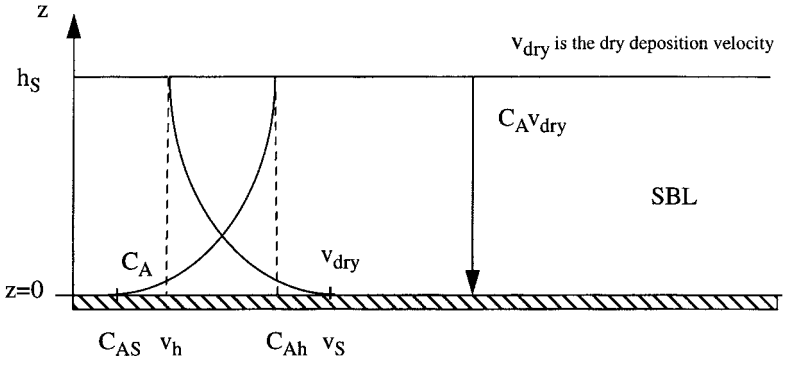

Fig. 1. The model for dry deposition.

irreversible. For the sulphur species this assumption seems to be well in agreement with the measurement data given by for example Fowler (1978), Garland (1978), McMahon and Denison (1979), Erisman et al. (1994) and references therein. According to Wesely (1989), a dry deposition module implemented in a regional scale model with a 50 km grid resolution can not be expected to produce accurate estimates of the dry deposition processes for short time periods at a particular small locations in the sub-grid area. Rather, the estimates in the present modeling are intended for long-term averages over at least a month or a year and for rather large areas over which the individual variations of land use compositions are smoothed.

Alternative dry deposition schemes have been proposed (Wesely, 1989; Erisman et al., 1994). In these schemes the surface deposition follows the resistance analogy, with an aerodynamic resistance (r_a) against turbulent transport down to the surface, an additional resistance against the diffusive transport through a thin layer adjacent to the surface (r_b) and finally a surface resistance accounting for uptake or destruction at the surface (r_s). The dry deposition velocity can be expressed in terms of the three resistances described above:

$$v_h = 1/(r_a + r_b + r_s). \tag{9}$$

In our parameterization: $v_s = 1/(r_s + r_b)$ and $r_a = 1/(C_H|v_H|)$.

Our formulation is thus in fact rather similar to the resistance parameterization, having an average value for the sum of r_b and r_s. In addition, according to Hicks et al. (1987), Wesely (1989) and Erisman et al. (1994) the uncertainty in the parameterization of r_s and r_b are considerable due to the limited knowledge concerning the physical mechanisms involved.

2.6. *Wet deposition*

The wet scavenging is calculated locally in each layer and summed in a column every time-step to obtain the deposition flux to the surface. The removal of sulphur in a layer is the product of the precipitation rate, the concentration in air and a dimensionless scavenging efficiency. The scavenging rates are based on a scavenging depth of 1000 m and the precipitation intensity within each layer. We do not account for the effect that dissolved material may be released when clouds or precipitation evaporates. The in-cloud and sub-cloud wet scavenging rates for sulphate and SO_2 components are similar to values utilized by Hobbs (1993) and Tarrason (1995, personal communication).

The scavenging efficiency for SO_2 has a seasonal sine wave variation throughout the year as in the Lagrangian model and it is expressed by

$$\Lambda_{SO_2} = \lambda_{SO_2} + \lambda\mathrm{amp}_{SO_2} \sin\left(2\pi\left(\frac{\tau - \tau_0}{\tau_a}\right)\right). \tag{10}$$

This formulation is included to account for the enhanced liquid phase formation and deposition of sulphate due to the higher concentrations of H_2O_2 in summertime than in wintertime. The loss of SO_2 due to wet deposition is calculated including the following sink term in the component continuity equation:

$$S_{SO_2,\ \mathrm{wet\ dep}} = -C_{SO_2} \frac{\Lambda_{SO_2} P}{\Delta z} \frac{1}{\rho_W}. \tag{11}$$

$\lambda_{SO_2} = 3{\cdot}10^5$ and $1.5 \cdot 10^5$ are the in-cloud and sub-cloud scavenging ratios respectively for SO_2. Furthermore, $\lambda\mathrm{amp}_{SO_2} = 1{\cdot}10^5$, τ is the time of the year (i.e., number of days since 1 January), τ_0 is 80 days, τ_a is one year, P is local precipitation intensity (kg m^{-2} s^{-1}), Δz is the scavenging depth assumed to be 1000 m and $\rho_W = 1000$ kg m^{-3} is the water density.

In the scavenging equation for sulphate (SO_4^{2-}) a similar sink term is used, where the in-cloud and sub-cloud scavenging ratios are $7{\cdot}10^5$ and $1{\cdot}10^5$ respectively. However, no seasonal variation is included for sulphate.

2.7. *Numerical methods and computational efficiency*

The time discretization of eq. (1) is performed with the fractional time step method (McRae et al., 1982). The different physical and chemical terms in the equation is then split into separate operations which are successively applied by intermediate time integrations. A central-difference scheme is applied for space discretization of the vertical diffusion. The model has been employed with a time-step of 5 min. The length of the time-step is limited by the Courant number in the vertical advection step due to the large number of layers close to the surface.

The present model simulations involve the solution of an advection-diffusion problem in three dimensions combined with sources and sinks for a full year. The resulting computational task would require weeks of CPU time on traditional sequential supercomputers, thus these simulations will benefit substantially from effective parallel algorithms.

Numerical algorithms, data structures and spatial data dependencies are important issues when parallelizing an existing code. It follows from the model formulation that the model contain only explicit advection dependencies in the horizontal directions, while the dependencies in the vertical are also implicit. Furthermore, the scavenging processes in the model have only vertical data dependencies, while the chemistry has no spatial dependencies. Based on the above information it was decided, as a first approach, to parallelize the model over the horizontal dimensions only. Further details on the theory behind the parallelization and the implementation to the present Eulerian model can be found in Skålin et al. (1995). In this paper it is demonstrated that the speed-up efficiency of the model performance is as high as 93% on 56 processors on an Intel Paragon distributed memory architecture.

2.8. Assimilation and boundary values

The model is run in a monthly cycle. The full three-dimensional model concentrations are stored at the end of each month and used to assimilate the preceding month. The first month will however be initiated on zero concentrations. At the lateral boundaries we have subjectively obtained values that correspond to seasonal averages calculated with the Hemispheric scale model for 1988 (Tarrason and Iversen, 1992). For the spring and the autumn we have utilized the same boundary values while separate values are used for the summer and the winter seasons. At the upper and lower boundaries it is assumed that the vertical turbulent and advective fluxes are equal to zero.

3. Meteorological, emission and surface data

3.1. Meteorological data

The multi-layer Eulerian air pollution model requires a large amount of meteorological input data. In order to overcome this requirement a dedicated version of the Operational Numerical Weather Prediction (NWP) model of The Norwegian Meteorological Institute (DNMI) has been set up. For a description of the NWP-model see Grønås et al. (1987) and Nordeng (1987). We will henceforth denote this particular version of the NWP-model for LAM50E (Limited Area Model, 50 km, Europe). The LAM50E is run in a six hourly intermittent data assimilation cycle with boundary values obtained from analysis made at the European Centre for Medium Range Weather Forecast. In the intermittent system observations from a period spanning the analysis time are used to correct a 6 hourly forecast made from the previous analysis. The analysis method is a modification of the successive correction method proposed by Bratseth (1986) and implemented for operational use at DNMI by Grønås and Midtbø (1987). A complete meteorological data set from a 6 hour forecast is then archived every 6 hours in 20 layers plus the surface layer. The most important meteorological parameters in the archive are described in Table 1.

The model domain has been selected to cover a region far enough away from the area of main interest, namely Europe, in order to avoid that the meteorological data would be significantly influenced by the boundary conditions. This is particularly important in the westward direction since many disturbances are entering Europe from the west. About ten model layers are placed below 2 km to obtain a high resolution of the boundary layer processes which are of special importance to the long-range transport of air pollution. The approximate heights above the surface of the model layers are given in the following assuming a standard atmosphere with a surface temperature of 288 K, a surface pressure of 1013 hPa and a vertical lapse rate of -6.5 K km^{-1}. The height of the lowest layer is approximately at 46 m. The heights of the following layers moving upwards are: 138 m, 236 m, 387 m, 586 m, 789 m, 996 m, 1207 m, 1434 m, 1688 m, 1961 m, 2578 m, 3611 m, 4770 m, 5095 m, 7235 m, 8642 m, 10 103 m, 11 891 m and 14 237 m. The meteorological data applied to the air pollution modeling between the 6 hourly intervals are found by linear interpolation.

3.2. Emissions

The emissions of SO_2 are based on officially reported 50 km values under the 1979 Geneva

Table 1. *The most important parameters included in the meteorological data archive*

Parameter	Output level	Parameter	Output level
U — x-component of wind	3-D	P — rate of precipitation release	3-D
V — y-component of wind	3-D	p_S — surface pressure	surface
$\dot{\sigma}$ — vertical velocity in σ-coordinate	3-D	H_S — surface flux of sensible heat	surface
θ — potential temperature	3-D	H_L — surface flux of latent heat	surface
q — specific humidity	3-D	τ — surface stress	surface
c_w — cloud liquid water	3-D	T_{2m} _ temperature at 2 m	surface

Convention on Long Range Transboundary Air Pollution as described in Berge et al. (1995). In areas where no official data exists 50 km × 50 km emission figures are either obtained from the emission compiled as a part of EU emission programmes, or, in areas with no existing information in the 50 km resolution at the time of the model runs, the 150 km emission numbers have been employed. This is the case for a large part of east-Europe and Russia. A distinction is also made between low level sources (below 100 m), and emission from tall chimneys (above 100 m), an information which is available from many European countries. Whereas low level sources are injected into the lowest model layer (below approximately 90 m), the remainder is injected to the 3 model layers immediately above, with 25% of the high emissions injected into layers 2 and 4 (from 90–180 and from 300–480 m respectively) 50% of the high sources are emitted into layer 3 (180–300 m). This is consistent with what is used in other European Eulerian air pollution models (Hass et al., 1990). Over the oceans, natural DMS emissions are given as monthly mean values. For the latest description of the estimates of DMS emissions the reader is referred to Tarrason et al. (1995). Finally, a seasonal variation in the source strengths follows a sine-function with an amplitude of 1.33 in January and 0.67 in July as presented in for example Barrett et al. (1995).

4. Presentation of results and discussions

The new model for long-term calculations of sulphur transport in Europe has been employed for the year 1992. The choice of 1992 was based on the fact that a complete and well quality checked three dimensional meteorological data set was available for this year. In the following sections we focus the presentation of the model results on the annual averaged quantities. The evaluation is made by on one side comparing the calculations with measurements. Mostly surface data has been available for the model evaluation. This is indeed unfortunate since the complete evaluation of the 3-D model would require vertically structured measurements as well.

On the other side we have compared with the results from the simpler two dimensional Lagrangian model of the EMEP program. This model has for many years been employed to long term calculations of transboundary fluxes and source-receptor matrices in Europe. A work supporting the development of emission reduction protocols under the 1979 Geneva convention on Long Range Transboundary Air Pollution.

4.1. Major weather patterns in 1992

In order to give a short overview of the weather patterns in 1992 we present the modeled averaged heights of the 1000 hPa and 500 hPa surfaces in July and January (Figs. 3a, b) and the spatial pattern of the total accumulated modeled precipitation for 1992 (Fig. 4). Average pressure and thickness fields for the whole year would not be very informative. Furthermore, the variation from season to season (not shown) was also in 1992 to a large degree characterized by the climatology of the region.

In January 1992 a high pressure was dominating over central and northwestern Europe. A strong jet-stream appears bending from the Atlantic Ocean northeastward to south of Iceland, and then further east and southeastward over Scandinavia to the Baltic Sea and western Russia. Frontal zones passed over northern parts of UK, Scandinavia and western Russia, while rather dry and stable conditions prevailed in central Europe.

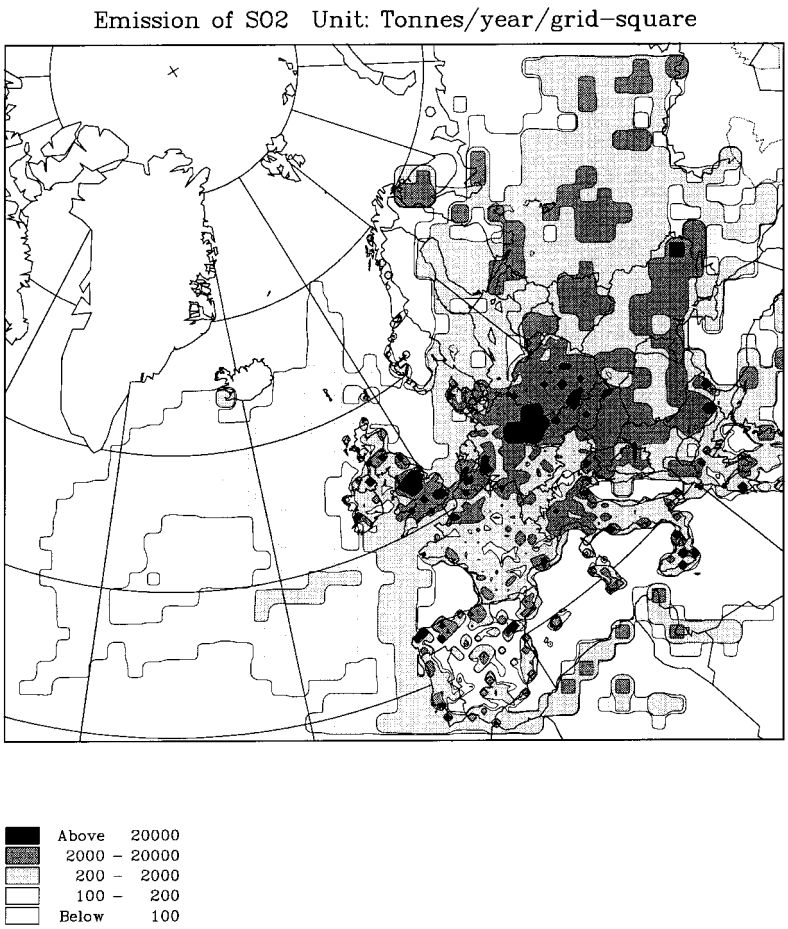

Fig. 2. Emission in tonnes of SO_2 per grid-square for 1992.

In July, however, the jet stream is much weaker and so are also the surface winds in northwestern Europe. The main high pressure system was moved west- and southwestward compared to January. Unstable air masses and frontal zones produced convective conditions with thorough vertical mixing and rather large amounts of precipitation in central and northern Europe.

The total accumulated precipitation for 1992 shows a large maximum east of North America between 40 and 50 N in the Atlantic Ocean. Other maxima are encountered in relation to mountain barriers for example the Pyrenees, the Alps and the Scandinavian mountains. Minimum areas are south and north of the polar front in the lee of mountain barriers and over the North Sea, the Baltic Sea and the Mediterranean Sea.

4.2. Concentration and deposition patterns in 1992

In Figs. 5a, b, the yearly average surface concentrations of SO_2 and SO_4^{2-} in air are presented. The highest annual averaged SO_2 concentrations of more than 20 $\mu g(S)\,m^{-3}$ are seen in Central-Europe and at a few other locations in UK and Spain. The lowest concentrations below 0.2 $\mu g(S)\,m^{-3}$ are found in the Atlantic Ocean, over Greenland and the polar areas. The maxima and minima of SO_4^{2-} coincide with the SO_2 pattern although less details are found since SO_4^{2-} is

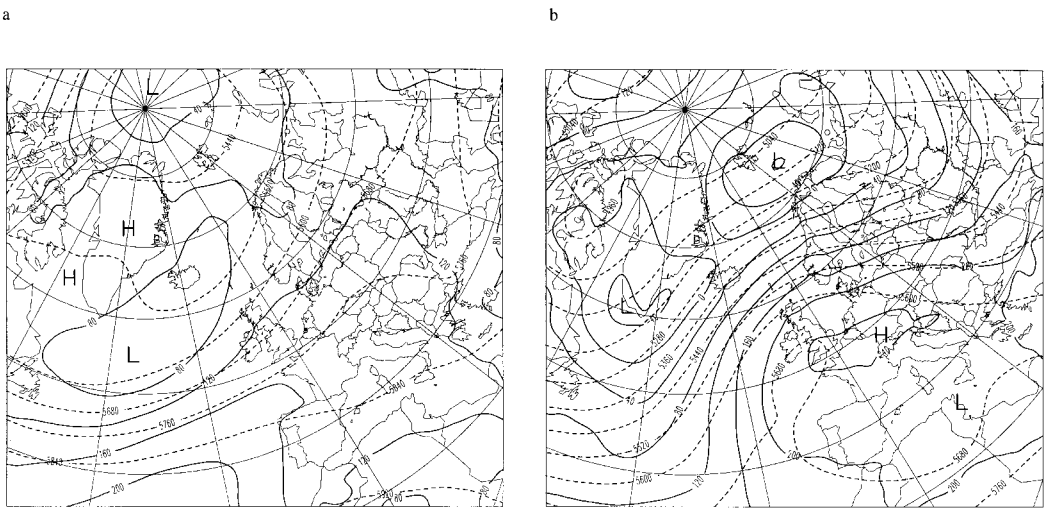

Fig. 3. (a) Averaged height (m) of the 1000 hPa surface (continuous line) and the 500 hPa surface (dashed line) for July 1992, and (b) averaged height (m) of the 1000 hPa surface (continuous line) and the 500 hPa surface (dashed line) for January 1992. Isolines are given every 40 m for the 1000 hPa surface and every 80 m for 500 hPa surface.

produced gradually after emission and it has a longer residence time in the atmosphere than SO_2. The highest sulphate concentrations are slightly above 4 μg(S) m^{-3}. The minimum values are encountered over Greenland and south-east of Greenland in the Atlantic Ocean and the Norwegian Sea. Increasing values toward the lateral boundaries are much more apparent than for SO_2. This resembles the boundary values introduced from the hemispheric scale model (see Subsection 2.8).

Furthermore, in Figs. 6a, b we present the accumulated dry and wet deposition respectively for 1992. As expected the dry deposition closely coincide with the surface concentration fields of SO_2 with a maximum near the main emitting areas. The wet deposition pattern reflects to a larger degree the transport and precipitation fields than only the magnitude of the surface concentration. The highest wet deposition rates are found in Central Europe in the main emitting areas. Furthermore, a maximum is seen in the Pyrenees, which is related to the large precipitation and the heavy emissions in north-western Spain (Fig. 2). Another maximum is encountered in the low emitting area of southern Norway. A further analysis of the wet deposition in southern Norway is given in the next section.

The annual figures of both concentration and deposition are qualitatively well in accordance with the simpler two-dimensional model (Barrett et al., 1995).

Finally, it is also interesting to note the quite large wet deposition in the western part of the Atlantic Ocean connected with the in-flux of sulphur through the western boundary and the large precipitation amounts in this area. The precipitation field (and consequently the sulphur deposition field) decreases somewhat toward the boundaries which is due to the relaxation zone near the boundary in the weather prediction model.

4.3. Comparison with measurements and a two-dimensional model

The monitoring sites utilized for the model evaluation are part of the EMEP monitoring network (Schaug et al., 1994) and their positions are given in Fig. 7. Scatter plots showing annual averages of the modelled versus observed values for SO_2, SO_4^{2-} and total wet deposition are presented in Figs. 8a, 9a and 10a, respectively. For reference the same results from the two-dimensional Lagrangian trajectory model operating at 150 km × 150 km model grid (Barrett et al., 1995) are given in Figs. 8b, 9b and 10b.

On an annual basis the results of the two models are rather similar for the air concentrations. There

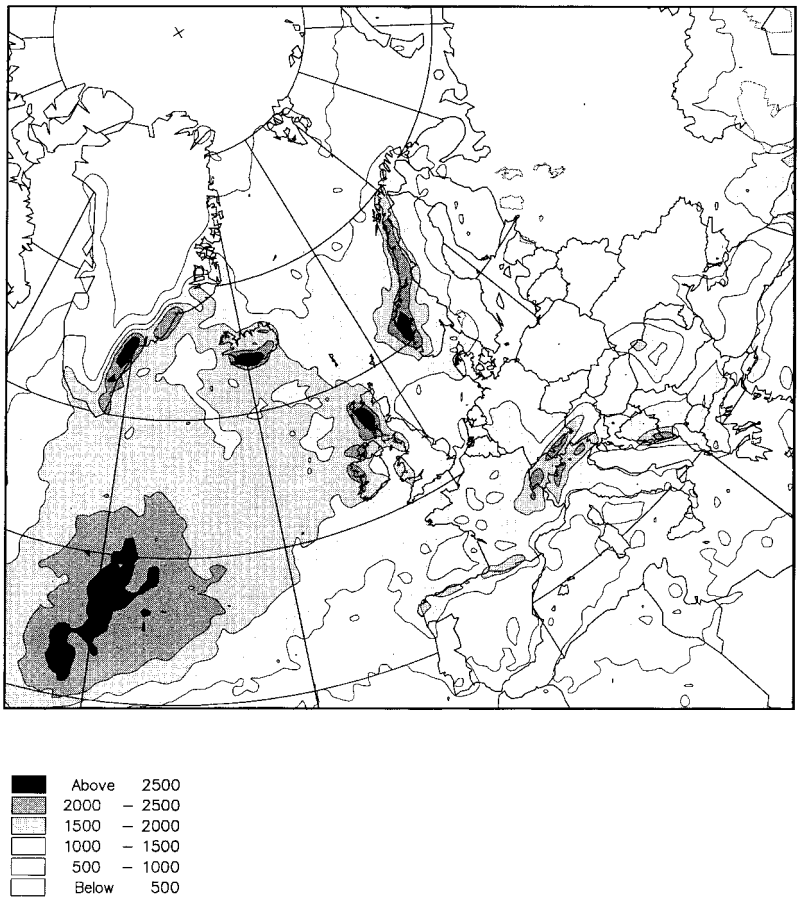

Fig. 4. Accumulated precipitation (mm) for 1992. Calculated with the weather prediction model. Isolines: 500, 1000, 1500, 2000 and 2500 mm.

is a tendency of the 3-D model to give slightly higher values on an average for SO_2, while somewhat lower values are encountered for SO_4^{2-} compared with the Lagrangian model. For SO_2 the number of stations with more than a factor of two deviation from the measurements is somewhat less for the multi-layer model. The same is true for sulphate in precipitation while the opposite is the case for sulphate in air. The averages over all stations are quite close to the observed average for both the models. The precipitation fields are in the Lagrangian model based on analysis of synoptic measurements over land areas interpolated to a 150 km model grid while the Eulerian model utilizes values from the Numerical Weather Prediction model described in Subsection 3.1. These two data sets are in Figs. 11a and b compared with the independent data set on accumulated precipitation from 61 EMEP-stations. A large scatter is found in both data set compared to the monitoring sites, and substantial differences are encountered at single stations. Averaged over all stations a good correspondence is found for both data sets. The data from the numerical weather prediction model then yields about 3% lower precipitation while the interpolation of synoptic measurement yields only slightly more than 1% higher value. On an annual basis there are therefore clear indications that the precipitation data originating from the numerical weather prediction model constitutes a good basis for the model calculations.

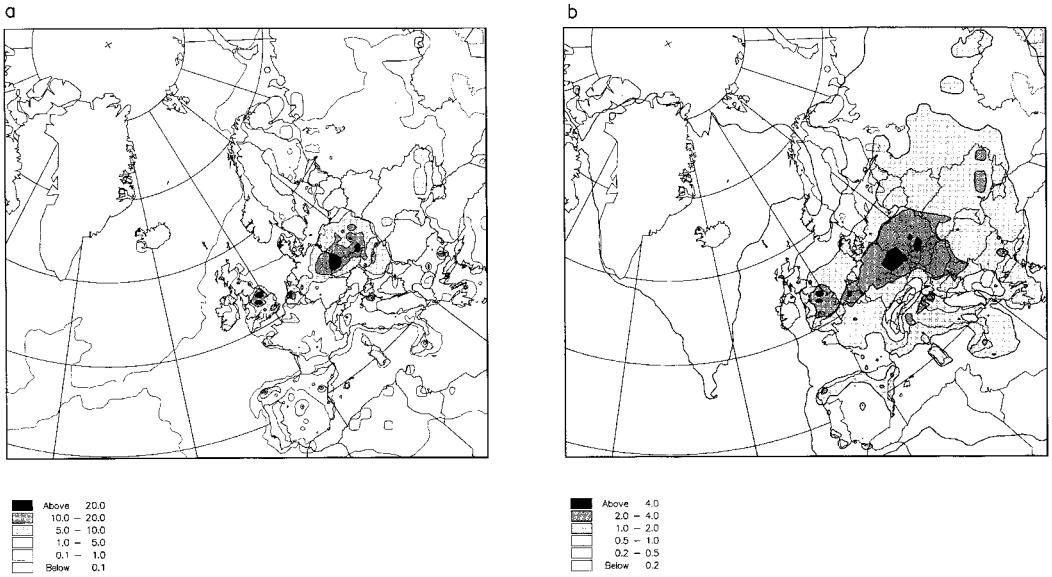

Fig. 5. (a) Yearly averaged concentrations in air of SO_2 ($\mu g(S)\,m^{-2}$) at ground level, for 1992. Isolines: 0.1, 1.0, 5.0, 10.0 and 20.0 $\mu g(S)\,m^{-3}$, and (b) yearly averaged concentrations in air of SO_4^{2-} ($\mu g(S)\,m^{-3}$) at ground level, for 1992. Isolines: 0.2, 0.5, 1.0, 2.0 and 4.0 $\mu g(S)\,m^{-3}$. Calculated with the Eulerian model.

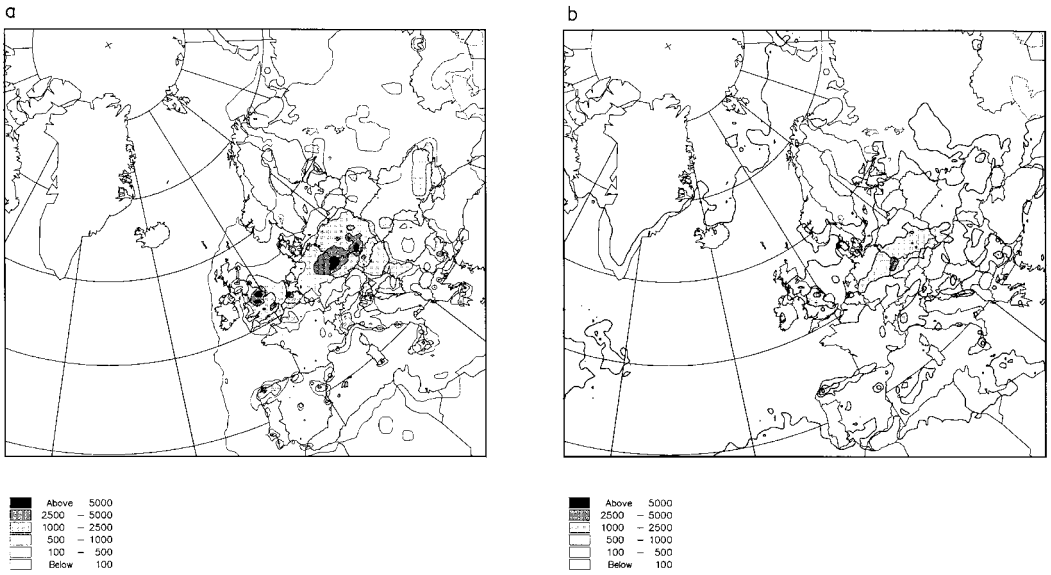

Fig. 6. (a) Accumulated dry deposition of sulphur ($mg(S)\,m^{-2}$) for 1992, and (b) accumulated wet deposition of sulphur ($mg(S)\,m^{-2}$) for 1992. Calculated with the Eulerian model. Isolines: 100, 500, 1000, 2500 and 5000 $mg(S)\,m^{-2}$.

We have examined the wet deposition in some further details over Norway by use of fields of sulphate concentration in precipitation interpolated to the 50 km grid. The method of interpolation is linear kriging and the methods and data used are described in Tørseth and Pedersen (1994). The kriged fields of sulphate in precipitation are obtained by combining 39 stations of

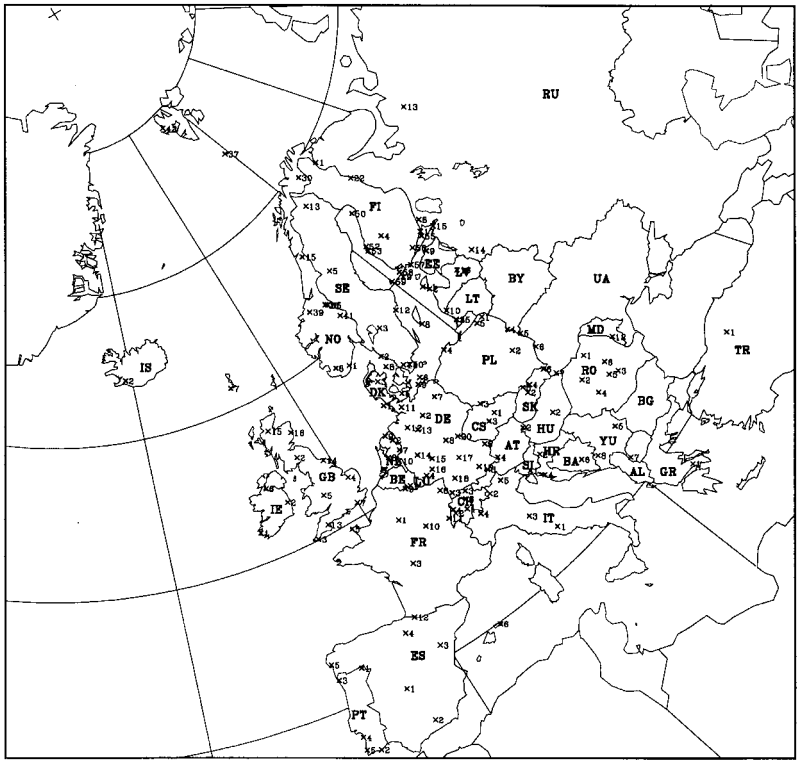

Fig. 7. The location of the EMEP monitoring sites in operation in 1992. The country codes applied are: AL-Albania, AT-Austria, BA-Bosnia and Herzegovina, BE-Belgium, BG-Bulgaria, BY-Belarus, CH-Switzerland, CS-Czech Republic, DE-Germany, DK-Denmark, EE-Estonia, ES-Spain, FI-Finland, FR-France, GB-United Kingdom, GR-Greece, HR-Croatia, HU-Hungary, IE-Ireland, IS-Iceland, IT-Italy, LT-Lithuania, LU-Luxembourg, LV-Latvia, MD-Moldova, NL-Netherlands, NO-Norway, PL-Poland, PT-Portugal, RO-Romania, RU-Russian Federation, SE-Sweden, SI-Slovenia, SK-Slovakia, TR-Turkey, UA-Ukraine, YU-Yugoslavia.

different Norwegian measuring programs. Use has also been made of Finnish and Swedish stations close to the Norwegian border. The accumulated deposition in each 50 km square is found by multiplying the concentration with the average annual precipitation in each square obtained from nearly 800 Norwegian precipitation stations.

Fig. 12a, b and c compare the accumulated sulphate deposition based on the kriged measurements, the multi-layer model and the Lagrangian model respectively. The Eulerian model yields rather good results for the interval (300–500) and (500–700) mg(S)/L in southern Norway. The peak deposition in southwestern Norway is however underestimated by as much as 30 to 40%. This can probably partly be ascribed to too low modeled precipitation values on the steep southwestern slopes of the mountains. However, the underestimation is much more pronounced in the Lagrangian model (Fig. 12c) in nearly all areas, including northern Norway. In central and eastern Norway the Lagrangian model yields 30–50% lower values than measured while the Eulerian model is quite close to the observed figures. Our conclusion is that the 3-D model gives improved calculations of the wet deposition of oxidized sulphur in most parts of Norway. The main reason for this improvement is most likely the inclusion of in-cloud scavenging together with an explicit treatment of the transport at higher levels (above the ABL) into the precipitating areas. The single level Lagrangian model, which describes the transport of air parcels extending up to the top of the ABL, can not resolve the above mentioned pro-

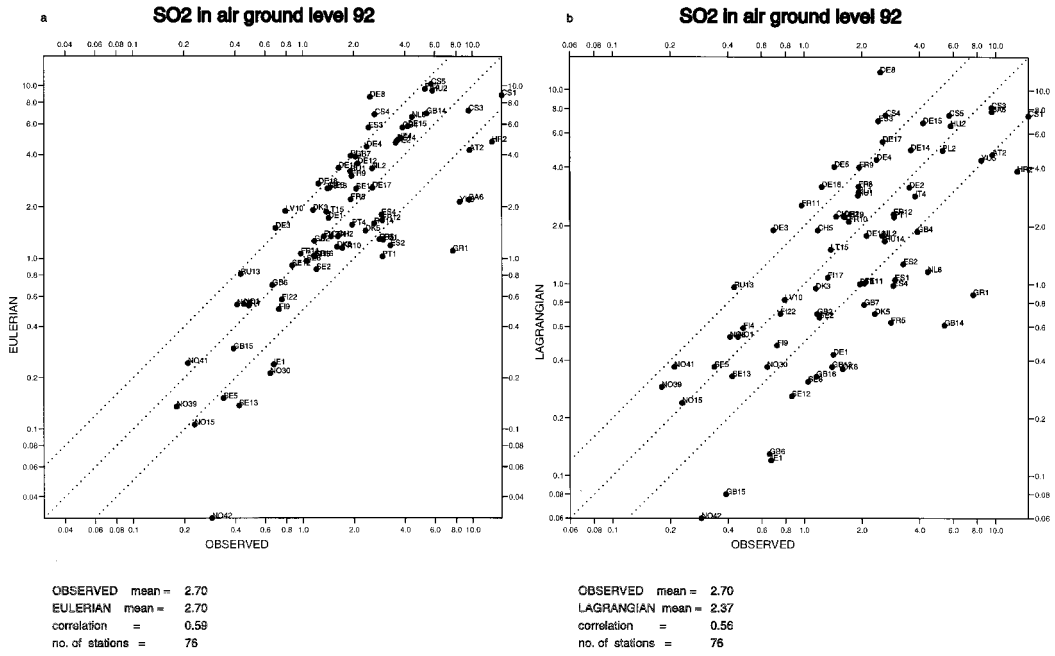

Fig. 8. Scatter plot of calculated and observed concentrations of SO_2 ($\mu g(S)\,m^{-3}$) in air at ground level (about 1 m height) for 1992 by use of (a) the Eulerian model, and (b) the Lagrangian model.

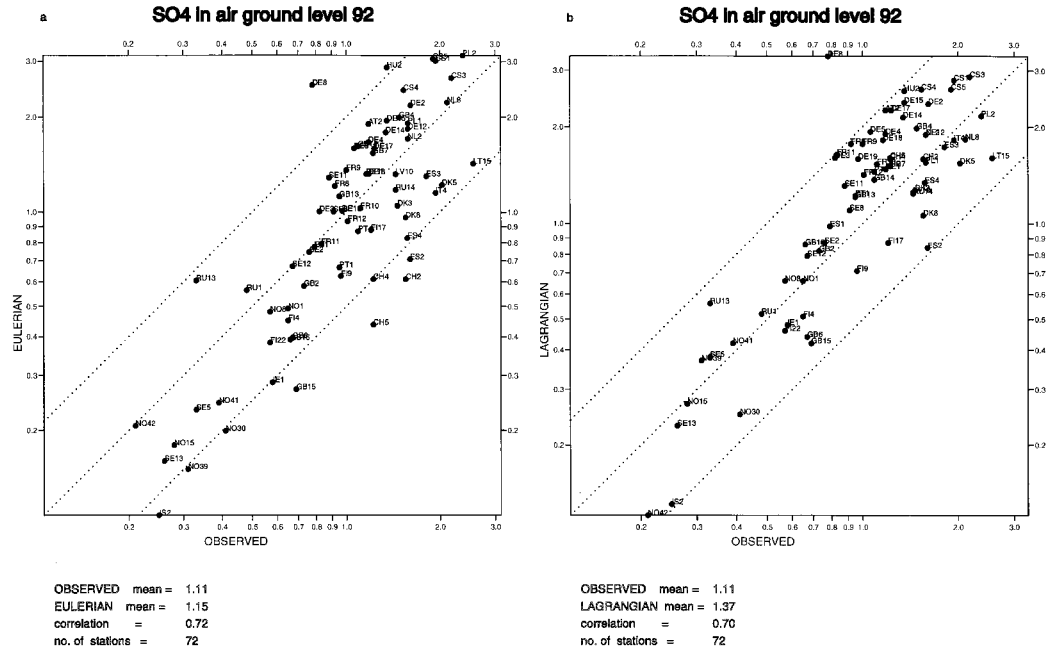

Fig. 9. Scatter plot of calculated and observed concentrations of SO_4^{2-} ($\mu g(S)\,m^{-3}$) in air at ground level (about 1 m height) for 1992 by use of (a) the Eulerian model, and (b) the Lagrangian model.

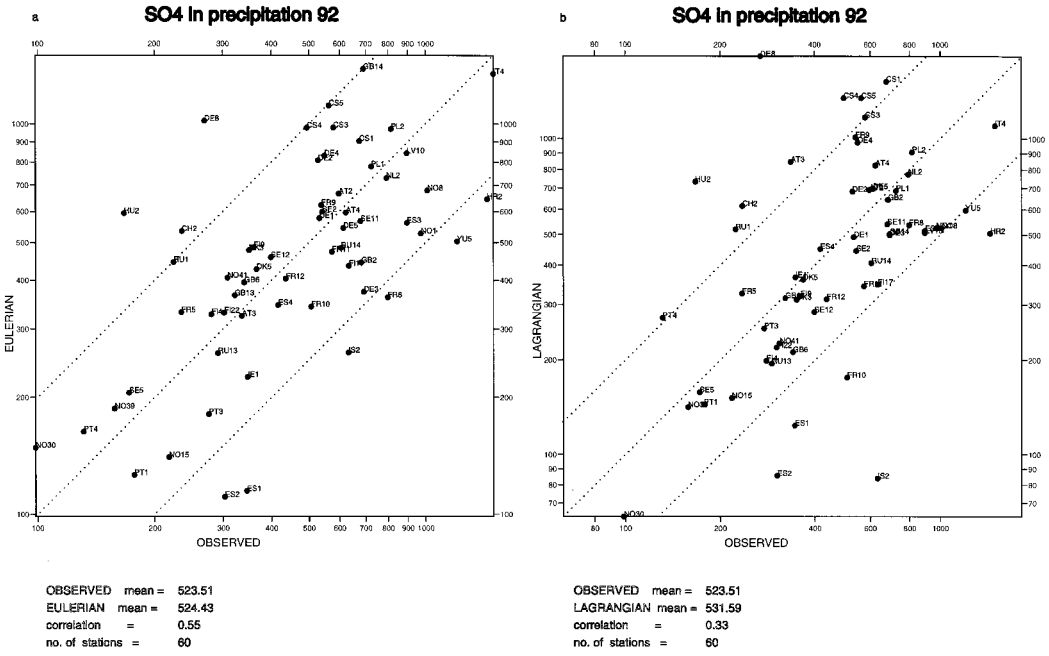

Fig. 10. Scatter plot of calculated and observed accumulated deposition of SO_4^{2-} in precipitation (mg(S) m^{-2}) for 1992 by use of (a) Eulerian model and (b) the Lagrangian model.

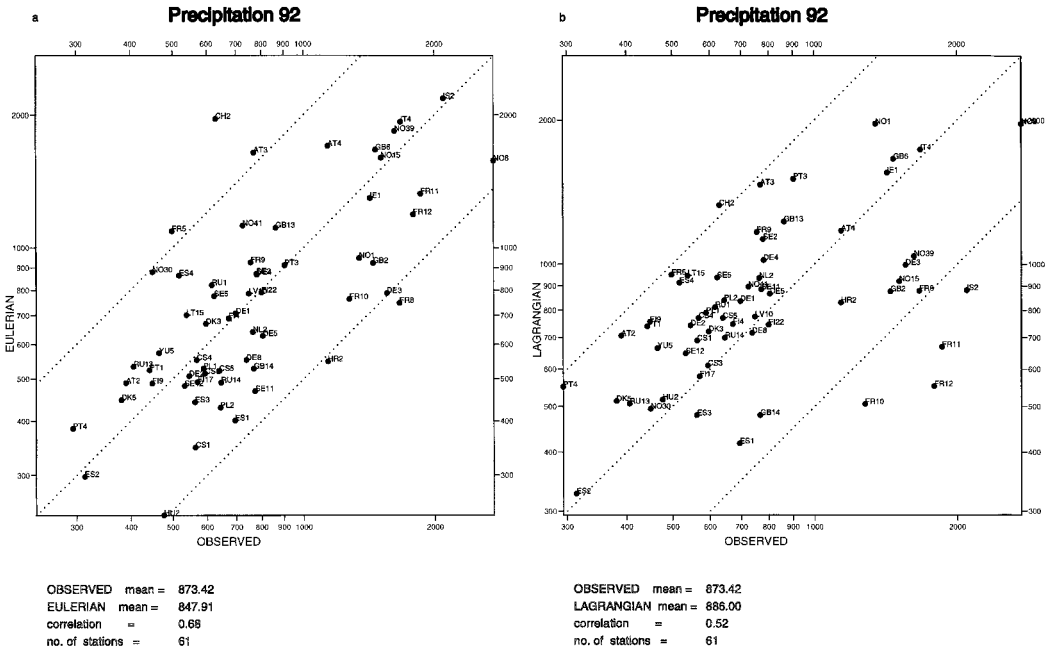

Fig. 11. Scatter plot of calculated and observed accumulated precipitation (mm) for 1992 by use of (a) the Eulerian model, and (b) spatial interpolation of synoptic measurements of precipitation.

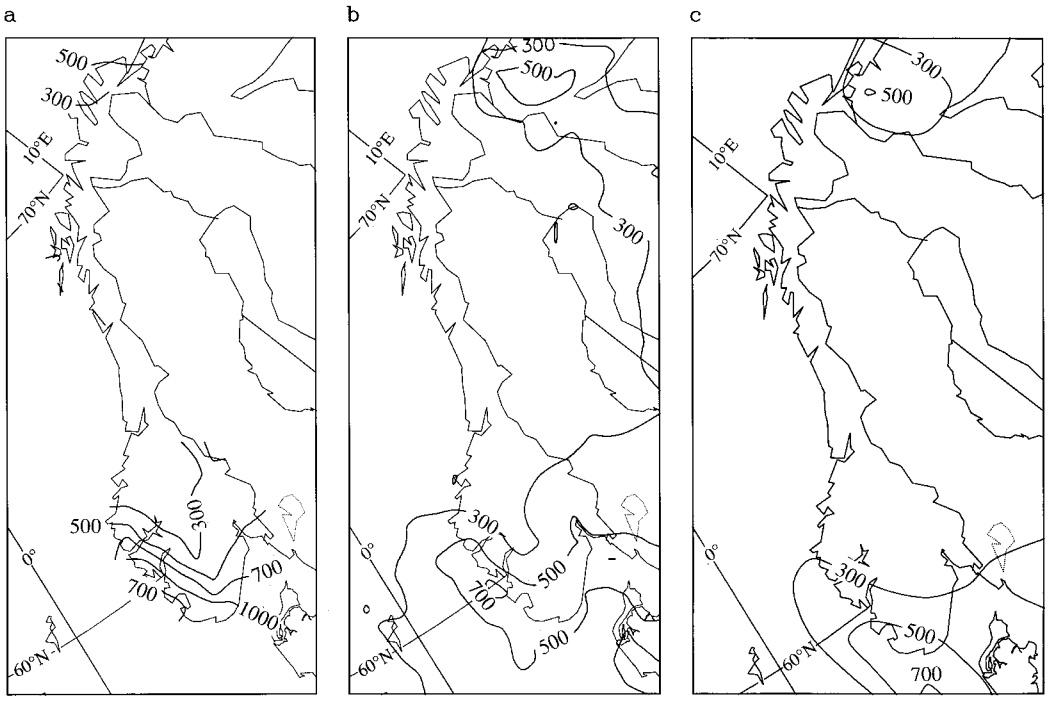

Fig. 12. Accumulated deposition of SO_4^{2-} in precipitation (mg(S) m^{-2}) for 1992 in Norway by using (a) annual kriged observed sulphur concentration fields, (b) the Eulerian model, and (c) the Lagrangian model. Isolines: 300, 500, 700 and 1000 mg(S) m^{-2}.

cesses and consequently the calculations become more uncertain.

Finally, we want to point out a couple of interesting features from the modelled fields in the Alps. First, from Figs. 5a, b we observed a minimum in SO_2 and SO_4^{2-} concentrations in the Alps. The Swiss EMEP station Jungfraujoch (CH 1) situated at 3573 m is representing average background tropospheric conditions in this area. The model surface has a height of approximately 2700 m in the grid-square coinciding with the position of CH 1. The modelled averages for 1992 are about 0.6 μg(S) m^{-3} for SO_2 and 0.4 μg(S) m^{-3} for SO_4^{2-} while the corresponding observations are about 0.2 and 0.4 μg(S) m^{-3} (Schaug et al., 1994). If we consider the model values at about 3500 m we find values of approximately 0.1 μg(S) m^{-3} and 0.2 μg(S) m^{-3} for SO_2 and SO_4^{2-} respectively. This indicates that the modelled tropospheric concentrations above central Europe are realistic although possibly somewhat underestimated.

Second, we would also like to highlight the minimum in the wet deposition over the Alps in between areas of larger wet deposition both at the northern and southern side of these mountains (Fig. 6b). A closer scrutiny of the fields show that there is a local minimum in the precipitation which coincides with the relatively low air concentrations. These two factors together give rise to rather low modeled depositions. Additional comparisons with CH 2 show that the wet deposition is somewhat overestimated at this station, while it compares well at AT 3 and AT 4. This indicates that the modeled minimum wet deposition is realistic.

4.4. *Mass budgets*

A monthly mass-budget is obtained by integrating the emission fluxes, the dry- and wet-deposition fluxes, and the fluxes in and out of the lateral boundaries. This has been worked out for the entire modeling domain presented in Fig. 3. The

size of this domain is approximately 4.8×10^7 km^2. The results are presented in Figs. 13a, b separated on SO_2 and SO_4^{2-}. The total emissions follow a sinusoidal prescribed distribution (see Section 3.2) with a maximum in January and a minimum in July. The integrated dry deposition of SO_2 follows closely the emission pattern, while the dry deposition of sulphate particles, which is much smaller than for SO_2 varies much less throughout the year. The wet deposition of SO_2 has a minimum from June to August. The maximum is found from February to April. The wet deposition of SO_4^{2-} is somewhat larger and it peaks in February. During the rest of 1992 no particular minimum or maximum is evident.

The fluxes across the lateral boundaries are larger in the winter season than in the summer season for both components due to stronger winds and higher concentrations. However, there are some more detailed features to be noted. The fluxes into the model domain is larger for SO_4^{2-} than for SO_2 and it is dominated by fluxes through the western boundary given by the hemispheric model. A large fraction of this import is wet deposited in the mid-Atlantic ocean as indicated by Fig. 6b. However, as shown by Tarrason and Iversen (1992) a significant part of the sulphur emissions in North America are also deposited along the western coastlines of Europe. In the wintertime the fluxes out of the domain for

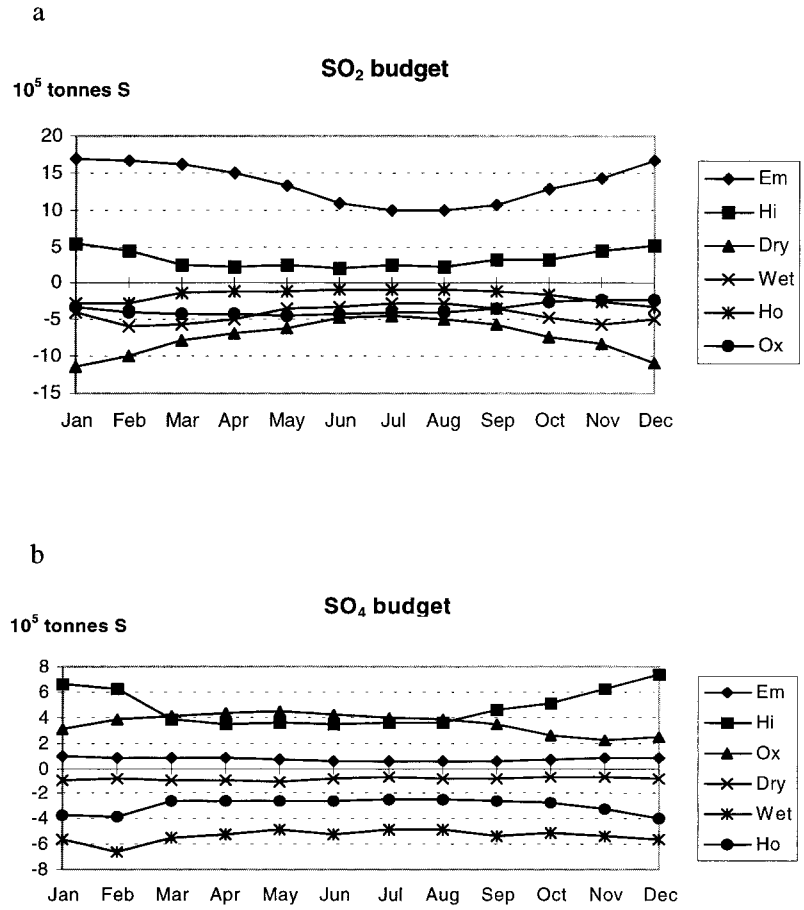

Fig. 13. Monthly mass budget for 1992 for (a) SO_2 and (b) SO_4^{2-} integrated over the entire modeling domain. Explanations: Em = emissions, Dry = dry deposition, Wet = wet deposition, Ox = oxidation from SO_2 to SO_4^{2-}, Hi = horizontal flux into the modeling domain and Ho = horizontal flux out of the modeling domain.

SO_4^{2-} and SO_2 are comparable while the outgoing transport will be dominated by sulphate in the summertime. This can be explained by the fact that SO_2 will have a larger residence time in the winter than in the summer due to lower chemical transformation rates. This is illustrated by the integrated oxidation from SO_2 to SO_4^{2-} which peaks in the late spring and early summer with nearly half a million tonnes of S per month. We further notice that about 50% of the emitted SO_2 is oxidized to sulphate in the summertime, while only about 20% is transformed during mid-winter.

The mass balance of the model is kept within 1–2% per month for the sum of SO_2 and SO_4^{2-}. The small deviations found are most likely due to minor inconsistencies in the interpolated meteorological data utilized in the air pollution model.

5. Summary and conclusions

In this paper we have presented a multi-layer model for the calculation of long term transport and deposition of air pollution in Europe. The model equations are formulated in the same grid system as the numerical weather prediction model utilized to generate the meteorological input data.

The basic input data to the model is a complete three-dimensional meteorological data set in a 50 km × 50 km grid horizontal resolution, and high resolution in the vertical (about 10 layers below 2 km). The emissions to the atmosphere are taken from the data officially reported to the Convention on Long Range Transboundary Air Pollution in Europe. For some parts of the modeling domain such emission data is not available, and other sources of data are then used.

The transport formulation of the model has been elaborated to include a higher order numerical advection scheme in order to minimize the numerical errors. The model makes use of simple parameterization schemes for the chemical transformation, and the dry and wet scavenging of air pollutants. The wet scavenging is calculated locally taking into account the precipitation releases and intensities.

Model comparisons with measurements show realistic values for both SO_2 and sulphate in air and sulphate in precipitation averaged over a year and for about 60–70 measuring stations in Europe. However, the deviations at individual measuring sites are often much larger, but seldom more than a factor of 2 difference is encountered.

The results are also compared with a simpler two-dimensional Lagrangian model with 150 km × 150 km resolution. Qualitatively, good consistency is found with the simpler model. However, significant differences are also encountered in particular in the deposition fields. A closer scrutiny of a large data set on wet deposition in Norway shows considerable improvements of the wet deposition with the multi-layer model compared with the two-dimensional boundary layer model. These improvements are most likely due to a more physically realistic description of the transport processes and the wet scavenging in the multi-layer model, which to a large extent also takes place above the boundary later.

The above presented results encourage the further development and application of the model to other chemical components than sulphur. Since the development of the model is a part of the EMEP program future applications in the field of policy oriented investigations are also foreseen.

6. Acknowledgements

The presented model runs have been carried out on a 56 processor Intel Paragon and on a CRAY Y-MP at the Technical University of Norway, Trondheim, Norway provided by the Norwegian Research Council. The authors are in particular indebted to Dr. Roar Skålin at the Technical University of Norway for his assistance in parallelizing the program code and facilitate the model runs. The authors would also like to acknowledge the many valuable discussions and suggestions from Professor Trond Iversen, University of Oslo, Norway during the development of new model. Finally, the authors would thank Mr. Anstein Foss and Mr. Egil Støren at the Norwegian Meteorological Institute for their assistance in preparing the figures, and Mr. Jan Schaug and Mr. Kjetil Tørseth at the Norwegian Institute of Air Research for providing measurements for the model evaluation.

REFERENCES

Amann, M. and Klaasen, G. 1995. Cost-effective strategies for reducing nitrogen deposition in Europe. *Journal of Environmental Management* **43**, 289–311.

Barrett, K. J., Seland, Ø., Foss, A., Mylona, S., Sandnes, H., Styve, H. and Tarrason, L. 1995. *European transboundary acidifying air pollution: 10 years calculated fields and budgets to the conclusion of the first sulphur protocol*. EMEP/MSC-W, Report 1/95. Norwegian Meteorological Institute, Oslo, Norway.

Berge, E. 1990. A regional numerical sulfur dispersion model using a meteorological model with explicit treatment of clouds. *Tellus* **42B**, 389–407.

Berge, E. and Kristjansson, J. E. 1992. Numerical weather simulations with different formulations for the advection of humidity and cloud water. *Mon. Wea. Rev.* **120**, 1583–1602.

Berge, E., Styve, H. and Simpson, D. 1995. *Status of the emission data at MSC-W*. EMEP/MSC-W Report 2/95. Norwegian Meteorological Institute, Oslo, Norway.

Blackadar, A. K. 1979. High resolution models of the planetary boundary layer. *Advances in Environment and Scientific Engineering*, 1. Gordon and Branch, 276 pp.

Bott, A. 1989a. A positive definite advection scheme obtained by non-linear renormalization of the advective fluxes. *Mon. Wea. Rev.* **117**, 1006–1015.

Bott, A. 1989b. Reply. *Mon. Wea. Rev.* **117**, 2633–2636.

Bratseth, A. M. 1986. Statistical interpolation by means of successive corrections. *Tellus* **38A**, 438–447.

Carmichael, G. R., Peters, L. K. and Kitada, T. 1986. A second generation model for regional-scale transport/chemistry/deposition. *Atmos. Environ.* **20**, 173–188.

Carmichael, G. R., Peters, L. K. and Saylor, R. D. 1991. The STEM-II regional acid deposition and photochemical oxidant model-1. An overview of model development and applications. *Atmos. Environ.* **25A**, 2077–2090.

Chang, J. S., Brost, R. A., Isaksen, I. S. A., Madronich, P., Stockwell, W. R. and Walcek, C. J. 1987. A three-dimensional Eulerian acid deposition model: Physical concepts and formulation. *J. Geophys. Res.* **92**, 14681–14700.

Dabdub, D. and Seinfeld, J. H. 1994. Numerical advection schemes used in air quality models — sequential and parallel implementation. *Atmos. Environ.* **28**, 3369–3385.

Eliassen, A. 1978. The OECD study of long range transport of air pollutants: Long range transport modelling. *Atmos. Environ.* **12**, 479–487.

Eliassen, A. and Saltbones, J. 1983. Modelling of long-range transport of sulphur over Europe: A two year model run and some model experiments. *Atmos. Environ.* **22**, 1457–1473.

Erisman, J. W., van Pul, A. and Wyers, P. 1994. Parameterization of surface resistance for the quantification of atmospheric deposition of acidifying pollutants and ozone. *Atmos. Environ.* **28**, 2595–2607.

Fowler, D. 1978. Dry deposition of SO_2 on agricultural crops. *Atmos. Environ.* **12**, 369–373.

Garland, J. A. 1978. Dry and wet removal of sulphur from the atmosphere. *Atmos. Environ.* **12**, 349–362.

Grønås, S., Foss, A. and Lystad, M. 1987. Numerical simulations of polar lows in the Norwegian Sea. *Tellus* **39A**, 334–352.

Grønås, S. and Midtbø, K. H. 1987. Operational multivariate analysis by successive corrections. *J. Meteorol. Soc. Jpn., WMO/IUGG/NWP, Symp.*, Special Issue, 61–74.

Hass, H., Jakobs, H. J., Memmesheimer, M., Ebel, A. and Chang, J. S. 1990. Simulation of a wet deposition case in Europe using the Eulerian Acid Deposition Model (EURAD). *18th ITM on air pollution modelling and its applications*, vol. 1, 153–160.

Hass, H., Ebel, A., Feldmann, H., Jakobs, H. J. and Memmesheimer, M., 1993. Evaluation studies with a regional chemical transport model (EURAD) using air quality data from the EMEP monitoring network. *Atmos. Environ.* **27A**, 867–887.

Hicks, B. B., Baldocchi, D. D., Meyers, T. P., Hosker, Jr., R. P., and Matt, D. R. A. 1987. Preliminary multiple resistance routine for deriving dry deposition velocities from measured quantities. *Water, Air, and Soil Pollution*, **36**, 311–330.

Hobbs, P. V. 1993. Aerosol-cloud-climate interactions, ed. Peter V. Hobbs: *International Geophysics*, vol. 54, Academic Press, San Diego, California, pp. 233.

Hov, Ø., Eliassen, A. and Simpson, D. 1988. Calculation of the distribution of NO_x compounds in Europe. In: *Tropospheric ozone* (edited by Isaksen, I. S. A.), pp. 239–261. D. Reidel, Dordrecht.

Iversen, T. 1993. Modelled and measured transboundary acidifying pollution in Europe—Verification and trends. *Atmos. Environ.* **27A**, 889–920.

Iversen, T. and Nordeng, T. E. 1987. *A numerical model suitable for the simulation of a broad class of circulation systems on the atmospheric mesoscale*. Techn. Rep. No. 2. Norwegian Institute For Air Research, Lillestrøm, Norway.

Louis, J. F. 1979. A parametric model of vertical eddy fluxes in the atmosphere. *Boundary Layer Meteorol.* **17**, 187–202.

McHenry, J. and Dennis, R. L. 1994. The relative importance of oxidation pathways and clouds to atmospheric ambient sulfate production as predicted by the regional acid deposition model. *J. Appl. Meteorol.* **33**, 890–905.

McMahon, T. A. and Denison, P. J. 1979. Empirical atmospheric deposition parameters. A survey. *Atmos. Environ.* **13**, 571–585.

McRae, G. J., Goodin, W. R. and Seinfeld, J. H. 1982. Numerical solution of the atmospheric diffusion equa-

tion for chemically reacting flows. *J. Comp. Phys.* **45**, 1–42.

Nordeng, T. E. 1987. The effect of vertical and slantwise convection on the simulation of polar lows. *Tellus* **39A**, 354–375.

Prandtl, L. 1942. Bermerkungen zur Theorie der freien Turbulenz. *Z. Angew. Math. Mech.* **22**, 241.

Rood, R. B. 1987. Numerical advection algorithms and their role in atmospheric transport and chemistry models. *Rev. Geophys.* **25**, 71–100.

Schaug, J., Pedersen, U., Skjelmoen, J. E., Arnesen, K. and Bartonova, A. 1994. *Data report 1992. Part 1: Annual summaries.* EMEP/CCC Report 4/94. The Norwegian Institute for Air Research, Lillestrøm, Norway.

Simpson, D. 1993. Photochemical model calculations over Europe for two extended summer periods: 1985 and 1989. Model results and comparison with observations. *Atmos. Environ.* **27A**, 921–942.

Simpson, D. 1996. Hydrocarbon reactivity and ozone formation in Europe. *J. Atmos. Chemistry* **20,** 163–177.

Skålin, R., Lie, I. and Berge, E. 1995. A parallel algorithm for simulation of long range transport of air pollution. In: *High performance computing in the geosciences* (F.-X. Le Dimet (ed)), pp. 175–185. Kluwer Academic Publishers, The Netherlands.

Tarrason, L. and Iversen T. 1992. The influence of north American anthropogenic sulphur emissions over western Europe. *Tellus* **44B**, 114–132.

Tarrason, L., Turner, S. and Fløisland, I. 1995. Estimation of seasonal DMS fluxes over the north Atlantic ocean and their contribution to European pollution levels. *J. Geophys. Res.* **100**, no. D6, 11623–11639.

Tørseth, K. and Pedersen, U. 1994. *Deposition of sulphur and nitrogen components in Norway 1988–1992.* Rep. OR 16/94. Norwegian Institute for Air Research, Postbox 100, N-2007 Kjeller, Norway.

Venkatram, A., Karamchandani, P. K., Kuntasal, G., Misra, P. K. and Davies D. L. 1992. The development of the acid deposition and oxidant model (ADOM). *Environ. Pollut.* **75**, 189–198.

Wesely, M. L. 1989. Parameterization of surface resistances to gaseous dry deposition in regional-scale numerical models. *Atmos. Environ.* **23**, 1293–1304.